COPY 1

Report No. FAA-RD-74-60

FEDERAL AVIATION ADMINISTRATION

OCT 21 1993

TECHNICAL CENTER LIBRARY
ATLANTIC CITY INT'L AIRPRT, NJ 08405

NAFEC
LIBRARY
JUN 3 '74
RECEIVED

Quarterly Technical Summary

ATC Surveillance/Communication Analysis and Planning

1 March 1974

Prepared for the Federal Aviation Administration by

Lincoln Laboratory

MASSACHUSETTS INSTITUTE OF TECHNOLOGY

LEXINGTON, MASSACHUSETTS

Document is available to the public through
the National Technical Information Service,
Springfield, Virginia 22151.

The contents of this report reflect the views of Lincoln Laboratory which is responsible for the facts and the accuracy of the data presented herein. The contents do not necessarily reflect the official views or policy of the Department of Transportation. This report does not constitute a standard, specification or regulation.

TECHNICAL REPORT STANDARD TITLE PAGE

1. Report No.	2. Government Accession No.	3. Recipient's Catalog No.
FAA-RD-74-60		

4. Title and Subtitle	5. Report Date
Quarterly Technical Summary ATC Surveillance/Communication Analysis and Planning	1 March 1974
	6. Performing Organization Code
7. Author(s)	8. Performing Organization Report No. QTS
9. Performing Organization Name and Address Massachusetts Institute of Technology Lincoln Laboratory P. O. Box 73 Lexington, Massachusetts 02173	10. Work Unit No. (TRAIS) 15434 022-243-012 & 033-241-062
	11. Contract or Grant No. IAG-DOT-FA72WAI-242
12. Sponsoring Agency Name and Address Department of Transportation Federal Aviation Administration Systems Research and Development Service Washington, D.C. 20591	13. Type of Report and Period Covered QTS 1 December 1973 – 28 February 1974
	14. Sponsoring Agency Code

15. Supplementary Notes

The work reported in this document was performed at Lincoln Laboratory, a center for research operated by Massachusetts Institute of Technology under Air Force Contract F19628-73-C-0002.

16. Abstract

FAA-funded ATC Surveillance/Communication Analysis and Planning activities during the period 1 December 1973 to 28 February 1974 are reported.

Under Task B, ASR Improvement Program, considerable progress has been made in bringing the hard-wired, full-coverage Moving Target Detector (MTD) to the operational stage. A minicomputer has been added to the system to display primitive aircraft reports, to test the MTD, and to measure radar stability. A test plan is being prepared for a comparison of the MTD with alternative radar systems at NAFEC. Preliminary analysis commenced on the application of an MTD-like processor to current magnetron-type ASRs. An advanced version of the feedback Clutter Mapper is being investigated.

Progress under Task D, which supports NAFEC programs ABIL, TPA, and E-Scan, continued. For ABIL, the real-time interrogator location program was completed and debugged except for the final phase of checkout with real data on the ABIL computer. A short new program for real-time computation of aircraft location with respect to a fixed ground point was also completed. In the TPA program, real-data tapes have been examined and work started on a program to calculate reflector locations from false target data on TPA and ARTS-III tapes. For the E-Scan antenna measurement program, additional analyses of false-target parameters and fading behind buildings were completed. In addition, there was significant participation in the development of the detailed test program for the E-Scan antenna measurements.

Construction of the PALM experimental system was completed and the antenna system installed on the antenna range during this quarter. The instrumentation system was also completed and installed in a mobile test van. Feasibility testing will commence in March.

17. Key Words		18. Distribution Statement
air traffic control	ABIL	Document is available to the public through the National Technical Information Service, Springfield, Virginia 22151.
surveillance	TPA	
clutter	E-Scan	
ATC radar	PALM	

19. Security Classif. (of this report)	20. Security Classif. (of this page)	21. No. of Pages	22. Price
Unclassified	Unclassified	28	3.00 HC 1.45 MF

Form DOT F 1700.7 (8-69)

CONTENTS

I. GENERAL 1

II. PRIMARY RADAR (ASR IMPROVEMENT PROGRAM, TASK B) 1

A. Introduction 1

B. FPS-18 Hardware, Exciter Improvement 3

C. MTD Hardware 3

1. Introduction 3
2. Description of MTD 5
3. MTD Hardware Status 7

D. NOVA Hardware, Fast Interfaces 7

E. NOVA Software 8

1. Data Simulation for MTD Testing 8
2. Data Entry and Display System Management 8
3. SGP Spectrum Analysis 8
4. Imlac Display Program 9

F. MTD Documentation 9

G. IOP Programming 9

H. NAFEC Test Plans 9

I. Feedback Clutter Mapper (FCM) 11

1. Design Considerations 11
2. Computer Simulation of FCM 13
3. Conclusions 13

J. Stability of Magnetron-Type ASRs 13

1. Magnetron Stability 14
2. Coho Stability 15
3. Stalo Stability 15
4. Other Stability Problems 15

III. NAFEC SUPPORT (TASK D) 15

A. Introduction 15

B. Airborne Beacon Interference Locator 15

1. Software Support 16
2. Real-Time Interrogator Location 16
3. Flight-Path Calculation 17

C. Transponder Performance Analyzer 17

D. E-Scan Antenna 18

IV. PRECISION ALTITUDE LANDING MONITOR (TASK E) 19

A. Introduction 19

B. Antenna Subsystem 20

C. Receiving System 20

D. Timing and Control System 23

ATC SURVEILLANCE/COMMUNICATION ANALYSIS AND PLANNING

I. GENERAL

This is the tenth ATC Surveillance/Communication Analysis and Planning Quarterly Technical Summary (QTS), covering the work performed by Lincoln Laboratory under Interagency Agreement DOT-FA72WAI-242 between the Federal Aviation Administration and the United States Air Force during the period 1 December 1973 to 28 February 1974.

During the period of this report, effort continued on the three tasks previously covered by the Agreement: Task B, ASR Improvement Program, Task D, NAFEC Support, and Task E, Precision Altitude and Landing Monitor. Progress on each of these tasks is reported below.

Also during the period of this report, Task F, Evaluation of Simulated Airborne Traffic Situation Display (ATSD) utilizing postulated ATCRBS, DABS, and Synchro-DABS data bases, was initiated. This evaluation is being conducted by a consortium of three on-campus M.I.T. Laboratories – the Electronic Systems, Flight Transportation, and Manned Vehicle Laboratories. Progress on Task F is reported by these Laboratories directly to the Office of System Engineering and Management by monthly letter reports and consequently will not be included in Quarterly Technical Summaries.

II. PRIMARY RADAR (ASR IMPROVEMENT PROGRAM, TASK B)

A. Introduction

The ASR improvement program has as its objective the development and demonstration of radar techniques which will improve the performance of ASR-type radars sufficiently to provide continuous, reliable data on all aircraft within their coverage patterns to automated control systems such as the ARTS-III.

The principal improvement to be demonstrated is an increase in subclutter visibility resulting from the introduction of advanced digital signal processing techniques. During the period August to November 1973, a limited-area version of a new digital processor called the Moving Target Detector (MTD) was demonstrated using Lincoln Laboratory's general-purpose, programmable Fast Digital Processor (FDP).

The FDP demonstration, although limited in coverage (8 nautical miles in range by 40 degrees in azimuth), successfully demonstrated the operation of the MTD concepts. This demonstration raised and helped to solve certain problems concerning thresholding and clutter overload. These problems were further addressed by exact simulation of the MTD digital processor on a bit-by-bit basis using an IBM-360 computer. Building on the results of the FDP demonstration and the simulation, the thresholding portions of the hard-wired MTD were largely redesigned and rebuilt. The full-coverage (48 nautical miles in range by 360 degrees in azimuth), hard-wired MTD has been completely checked out internally except for the operation of its output circuitry. This checkout is awaiting completion of the fast interface to the NOVA computer. This computer will be used to process the radar output for display on an ARTS-III Data Entry and Display System (DEDS), to routinely test the performance of the MTD, and to measure the stability of the radar.

During the next quarter, it is anticipated that the fast interface to the NOVA will be completed, the NOVA software finished and checked out, and the MTD placed in operation.

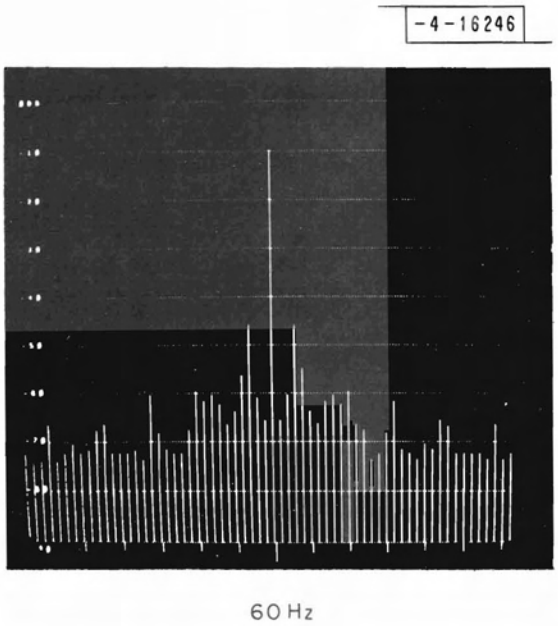

Fig. 1. Spectrum of original FPS-18 exciter (±500 Hz) in the variable prf mode.

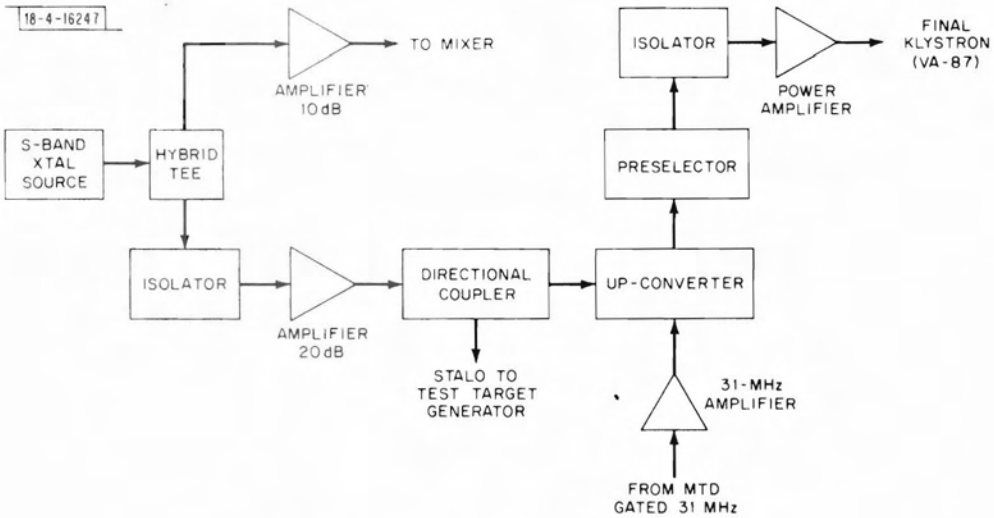

Fig. 2. Block diagram of new exciter.

In anticipation of the movement of equipment to NAFEC near the end of the coming quarter, work is now in progress to prepare for installation of the radar and ancillary equipment at NAFEC. Documentation is being prepared to completely describe the MTD radar system in order to facilitate maintenance and future modifications. UNIVAC is under contract to the FAA to write programs for the IOP computer (input/output processor of ARTS-III) to suitably combine and interpolate digital radar target reports from the MTD and to record and display them. Finally, a test plan is being written to guide the testing of the MTD radar at NAFEC. This work is described in some detail.

A device for normalizing the clutter level by providing feedback to the input attenuator is described. The new device is called a Feedback Clutter Mapper (FCM). A final item in this report is a description of work in progress to study the application of an MTD-like processor to a magnetron-type ASR. This includes an outline of proposed stability measurements on magnetron ASRs. Further work to improve magnetron ASRs will be carried on under Task G.

B. FPS-18 Hardware, Exciter Improvement

As previously reported (1 December 1973 QTS), the FPS-18 exciter originally consisted of two 3-cavity power klystrons with their ancillary pulser circuits. This exciter was designed to operate at a very stable fixed prf. When a variable prf was applied, adverse effects of the change in duty ratio were observed. Figure 1 shows the output spectrum (±500 Hz) of the original exciter, fed with a clean CW signal sampled at a variable prf. Effort to modify the existing system made it evident that it would be more prudent and economical to provide a new exciter.

The new exciter (Fig. 2) consists of an S-band crystal-controlled source whose output is fed to a hybrid tee so that part of the source is amplified and sent to the mixer preamplifier where it is heterodyned with the incoming target returns to produce a 31-MHz IF. The other output of the hybrid tee is amplified and fed to an up-converter to generate the transmitted signal. The gated 31 MHz is generated in the MTD.

The output of the up-converter is fed to a preselector which is tuned to the desired transmitter frequency. This output is amplified by a power amplifier which in turn drives the final klystron.

Figure 3 shows the spectral results when using the new exciter stage. The gain setting is the same as in Fig. 1. It is apparent from comparing Figs. 1 and 3 that the new exciter is a significant improvement. Figure 4 depicts the output of the new exciter with 10 dB more gain than in Fig. 3. At this setting, the central line (approximately 0 dB) is folded over and appears as shown. The contributions of the new exciter to stability sidelobes are now below the receiver noise level.

The klystron transmitter requires further improvement for variable prf operation. The areas that require improvement can now be analyzed since the spectral imperfections are no longer masked by the exciter instability noise.

C. MTD Hardware

1. Introduction

Before describing the MTD (Moving Target Detector), it is useful to describe some of the characteristics of the radar and radar data that it will process.

The FPS-18 is a mechanically scanning, S-band radar which will operate at variable prf (1240 ± 130 Hz). The scan sequence of the radar will consist of alternately transmitting

-4-16248

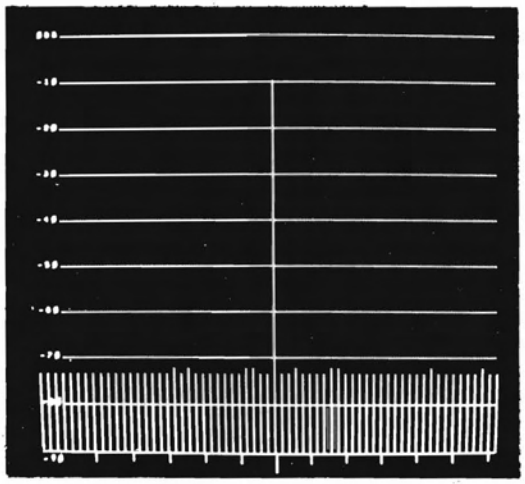

Fig. 3. Spectrum of solid state exciter in variable prf mode (±500 Hz).

-4-16249

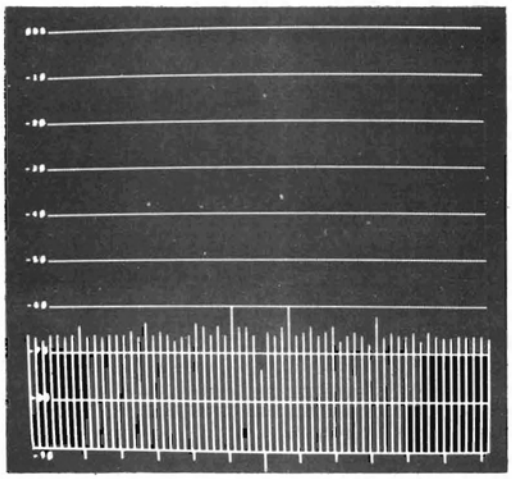

Fig. 4. Same as Fig. 3 but with 10 dB more gain. All lines are more than 60 dB below the carrier.

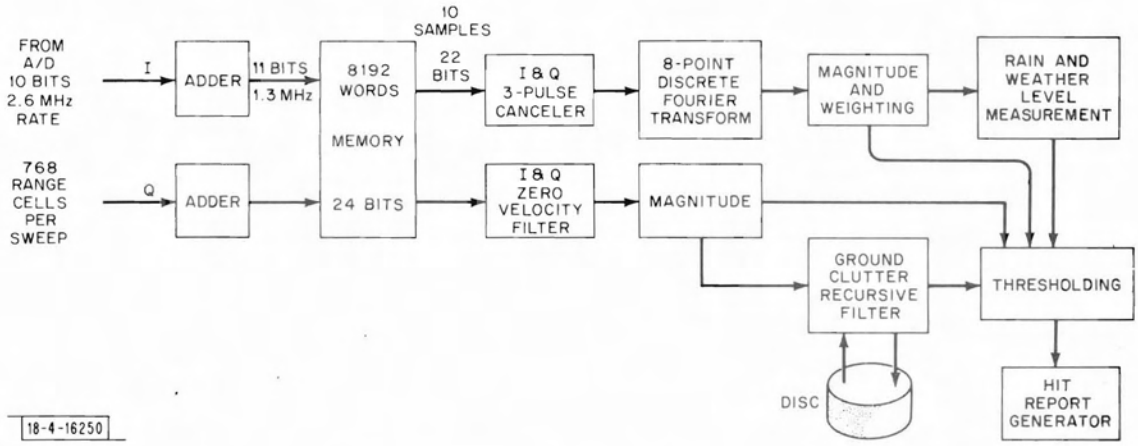

Fig. 5. MTD processor.

ten pulses at a constant "high" prf (1379.4 Hz), ten pulses at a "low" prf (1120.8 Hz), followed by typically two pulses (which are not processed) at the average prf. The "high" and "low" prf transmissions are used to resolve velocity ambiguities. On successive scans of the antenna, the "high," "low," and average prf's are altered slightly (1366.7, 1113.1, and 1232, respectively) to resolve range ambiguities. The 774-nsec pulse sampling time corresponds to about a 1/16 nmi range cell. Each sweep is sampled 760 times in 600 μsec.

2. Description of MTD

The MTD processor is a special-purpose, hard-wired signal processor which will be capable of processing the full 360° coverage of the FPS-18 radar out to a nominal range of 48 nmi.

The processor is designed to give optimum response to the expected signals and clutter backgrounds. The MTD response will be within 1 or 2 dB of the theoretical response obtainable with an optimum processor.* †

A block diagram of the processor is presented in Fig. 5. The I&Q (In-phase and Quadrature) signals are sampled at a 2.6 MHz rate by 10-bit A/D converters. The I&Q channels are then added coherently, two at a time, to produce 11-bit I&Q channel words at a 1.3-MHz rate. Ten consecutive samples of both the I&Q channels for each of 768 range gates (48 miles of range) are stored in a 8192-word, 24-bit memory. The I&Q channel samples are stored in two 11-bit sections of each 24-bit word; two bits are not used.

These 7600 words of the 8192-word memory are then processed sequentially (ten time samples for each range cell) by a 3-pulse MTI canceler. The I&Q channels are processed by separate hardware in the 3-pulse canceler section of the processor. Note that the ten pulses of 11-bit I&Q channel samples exist after the 3-pulse canceler as eight pulses of 13-bit words. The output of the 3-pulse canceler for both the I&Q channels (real and imaginary parts of the signal) is fed into an 8-point Discrete Fourier Transform (DFT) which produces eight Doppler cells.

Weighting of the I&Q channel signals to reduce the sidelobe level is done after the DFT. The weighting used is

$$I(f_i) = -\frac{1}{4} I(f_{i-1}) + I(f_i) - \frac{1}{4} I(f_{i+1})$$

and

$$Q(f_i) = -\frac{1}{4} Q(f_{i-1}) + Q(f_i) - \frac{1}{4} Q(f_{i+1}) \quad .$$

This is equivalent to a Hamming Weighting (cosine squared plus a $\frac{1}{4}$ pedestal) done before the DFT. Since weighting before the DFT would require multiplication, the weighting is done in the frequency domain as above because this implementation requires only addition (the multiplications by $\frac{1}{4}$ or any fractional power of 2 can be done by shifting of registers).

Since the 3-pulse canceler has poor low Doppler velocity response, a zero velocity filter (ZVF) is employed to see low radial velocity targets. This low-pass filter is implemented by coherently adding the first five samples of each of the I and Q channels, respectively, taking

---

* "ATC Surveillance/Communication Analysis and Planning," Quarterly Technical Summary, FAA-RD-73-35, Lincoln Laboratory, M.I.T. (1 March 1973).

† C. E. Muehe, et al., "Concepts for Improvement of Airport Surveillance Radars," Project Report ATC-14, FAA-RD-72-148, Lincoln Laboratory, M.I.T. (26 February 1973).

their magnitude and adding to this the magnitude of the sum of the last five samples. Thus,

$$ZVF = M_1 + M_2 \quad ,$$

where

$$M_1 = \text{Magnitude} \left\{ \sum_{i=1}^{5} I_i, \sum_{i=1}^{5} Q_i \right\} \quad ,$$

and

$$M_2 = \text{Magnitude} \left\{ \sum_{i=6}^{10} I_i, \sum_{i=6}^{10} Q_i \right\} \quad .$$

This gives a somewhat broader frequency response than simply adding coherently all ten samples and then taking the magnitude.

The magnitudes of the signals which come out of the 3-pulse canceler, DFT, and weighting chain are then taken. The magnitude of the signal $\{I, Q\}$ is approximated by

$$\text{larger of} \left\{ |L| \text{ and } \{\tfrac{7}{8}|L| + \tfrac{1}{2}|S|\} \right\} \quad ,$$

where $|L|$ is the larger of $|I|$ and $|Q|$, and $|S|$ is the smaller of $|I|$ and $|Q|$.

After magnitudes are taken, adaptive background levels and thresholds are set and threshold crossings (detections) are noted and output. The adaptive background levels and thresholds are set depending on the clutter phenomenon which is present. The Doppler domain is divided into three domains.

a. Doppler Cell 0

In this cell the clutter is generally due to ground backscatter. The average ground backscatter cross section varies from range-azimuth cell to range-azimuth cell. The average backscatter signal level for each cell is measured and stored on the disc (see Fig. 5). A recursive filter is used to update on a scan-to-scan basis the average signal level stored on the disc. On each scan, 1/nth of the stored clutter level is subtracted from the stored level. One nth of the signal level output from the ZVF is added to the value remaining after subtraction. This new level is then stored on the disc for thresholding in the next scan. The threshold for the 0 Doppler cell is a fixed value between 8 and 16 times the level stored on the disc. This fixed value may be altered by use of a wire jumper on the hardware.

b. Doppler Cells 2 Through 6

In these cells the clutter is due chiefly to rain. For each Doppler and angle cell, the average signal level is measured by averaging the received signal over 16 range cells (one mile) centered on the range cell of interest. The threshold for these cells is a fixed value set at four to eight times the measured average signal level.

c. Doppler Cells 1 and 7

These cells can contain clutter due to rain or spillover from the ground backscatter in cell 0. The threshold set in these cells is the greater of two thresholds: (a) the threshold set as in

Doppler cells 2 through 6, or (b) a fixed binary fraction [($\frac{1}{2}$n) n = integer] of the threshold set in cell 0. n is set by use of a wire jumper on the hardware.

Finally, it must be noted that if the I or Q channel sample is noted to have all the bits on (i.e., be in saturation), then any target detections for that range cell are deleted.

3. MTD Hardware Status

Extensive reconstruction and debugging of the MTD equipment took place during this quarter. A computer simulation of the MTD was written (see 1 December 1973 QTS) which indicated that some of the algorithms used in threshold generation were faulty, and that the clutter values stored on disc memory required greater accuracy than was possible with the 10 bits available. As a result, it was necessary to redesign the entire thresholding and disc interface portions of the hardware.

Since the new design requires that the clutter values be stored on the disc in floating-point format, floating-to-fixed-point and fixed-to-floating-point converters were included in the disc interface.

The MOS shift registers designed for the disc buffer memory were not available and had to be replaced with a substitute type. Since the longest shift registers which were available could accommodate only one-fourth as many bits as those in the original design, the disc buffer was expanded from 60 integrated circuits to 240 integrated circuits. This expansion resulted in the need for more DC power than was previously provided so new power supplies were ordered and installed.

As an aid in checkout and debugging, miniature digital-to-analog converters were built into several sections of the MTD. These are 10-bit, 1-MHz units which plug directly into a DIP circuit socket and are extremely compact.

All the aforementioned modifications have been completed and debugging has commenced. All portions of the system with the exception of the input/output processor (IOP) interface have been checked out. It is anticipated that the MTD radar will be fully operational and moved to NAFEC in the next quarter.

D. NOVA Hardware, Fast Interfaces

The NOVA system and its functions were described in the 1 December 1973 QTS. All hardware and peripherals ordered from Data General, except the hardware multiply/divide option, are on hand and working (see Fig. 6). The multiply/divide option is expected momentarily.

In addition to the above hardware, a high-speed multichannel interface is required. This is being designed and built by Lincoln Laboratory. At present, it is completely wired and is being checked out.

The high-speed multichannel interface services the following:

(1) MTD output words (32-bit target reports) are buffered, converted to two 16-bit words and input to NOVA.

(2) Two 16-bit NOVA words are converted to 32-bit words and passed on to the DEDS.

(3) The SGP 11-bit output for each quadrature video channel of the MTD is passed on to the NOVA in two 16-bit words.

(4) Two 16-bit NOVA words are converted into one 22-bit word and passed on to an 8000-word auxiliary memory used to hold data for testing the MTD.

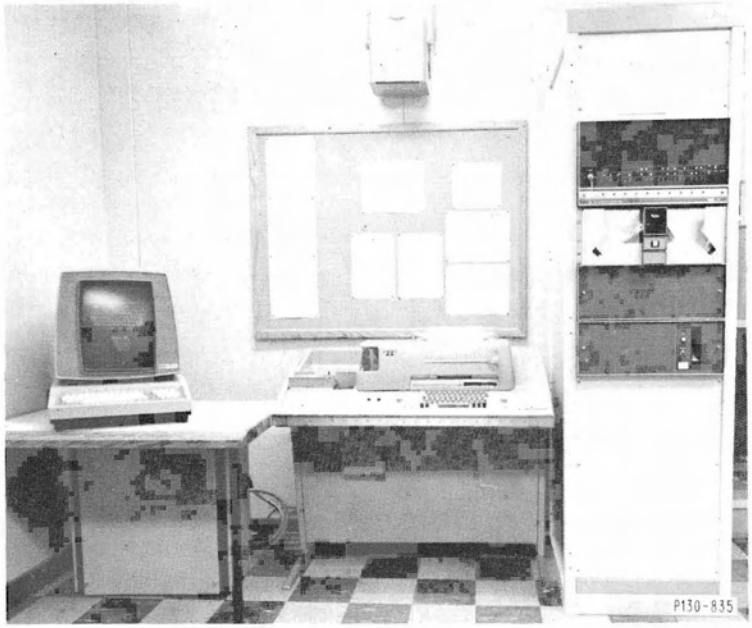

Fig. 6. NOVA computer system. From left to right: Imlac PDS-1 display, teletype ASR-35, NOVA 1200 computer, fast paper tape reader and fast paper tape punch.

E. NOVA Software

1. Data Simulation for MTD Testing

This program is designed to read blocks of radar data from paper tape, set up the appropriate buffers, and send an entire CPI (Coherent Processing Interval) of data to the auxiliary 8K memory at the beginning of each scan. Real-time comparison between the expected and actual MTD output is performed as an option. Results of the comparison are output to either the high-speed paper tape punch or the Imlac display.

All major portions of this program are designed, coded, and assembled. System debugging will be completed in the next quarter.

2. Data Entry and Display System Management

The DEDS management program is a two-part program designed to provide a scan history of radar targets on an ARTS-III PPI display (see 1 June 1973 QTS).

All sections of this program are designed, coded, and assembled. Documentation is nearly complete. On-line debugging will be completed in the next quarter.

3. SGP Spectrum Analysis

The Single Gate Processor (SGP) provides a real-time spectral display of the return from a single range-azimuth cell (see 1 March 1973 QTS).

The SGP program is 80 to 85 percent complete. Missing portions are primarily input/output sections and data formatting. On-line debugging will be completed in the next quarter. Documentation is in progress.

4. Imlac Display Program

The Imlac display program which will display the SGP output in graphic form, as well as several lines of alpha-numerics, has been contracted to an outside consultant. Design is complete and the program is partially coded. The program will be ready for integration into the over-all system in the next quarter.

F. MTD Documentation

Formal documentation of the modifications to the MTD radar commenced in this quarter. These modifications include a new receiver, radar exciter, signal processor (MTD), computer test facility (NOVA) and test target generator. A detailed functional system block diagram has been drafted and is being refined. Using this detailed functional block diagram, a drawing index has been prepared which is the basic guide for the documentation effort.

G. IOP Programming

The UNIVAC Division of Sperry Rand, under contract to the FAA, is developing an ARTS-III IOP target report correlation and interpolation program similar to that described in the 1 June 1973 QTS, which was for execution in the Raytheon 706 computer. Formal presentation of the program design was held at Lincoln Laboratory on 17 January 1974. The program being developed meets all requirements and is on schedule.

The program will collect the threshold crossings from the MTD, group the crossings that relate to a single target, calculate a refined target size, range, azimuth and velocity from the associated data, and pass this target report along for display and/or tracking update.

Sections of the program will also extract useful target information and record it on magnetic tape for later analysis and comparison with the ASR-7/RVD-4 data at NAFEC.

H. NAFEC Test Plans

Part of Lincoln Laboratory's responsibility under Task B is to prepare a plan for the testing of the MTD radar system at NAFEC. To that end, a meeting was held at Lincoln Laboratory on 7 February 1974. The meeting was attended by representatives from Lincoln Laboratory, NAFEC, UNIVAC, and SRDS. At that meeting, a test philosophy and an outline of the test plan were developed.

The purpose of the tests is to evaluate the FPS-18/MTD radar system for use as a sensor in an automated terminal radar control system. It has been decided that the test will be conducted as a comparison between the FPS-18/MTD system and the ASR-7/RVD-4 system in various clutter situations.

One of the prime criteria for distinguishing the two radar systems will be the continuity and lifetime of the tracks formed on aircraft and the rate of production of false tracks. Tests will involve both synthetic targets and aircraft of all sizes, aspect angles, and speeds under a wide variety of clutter conditions.

An outline of the test plan was prepared and is being distributed. It includes five major headings – namely, Introductory Material, Test Quality Assurance Provisions, Synthetic Target Tests, Flight Tests, and Data Analyses.

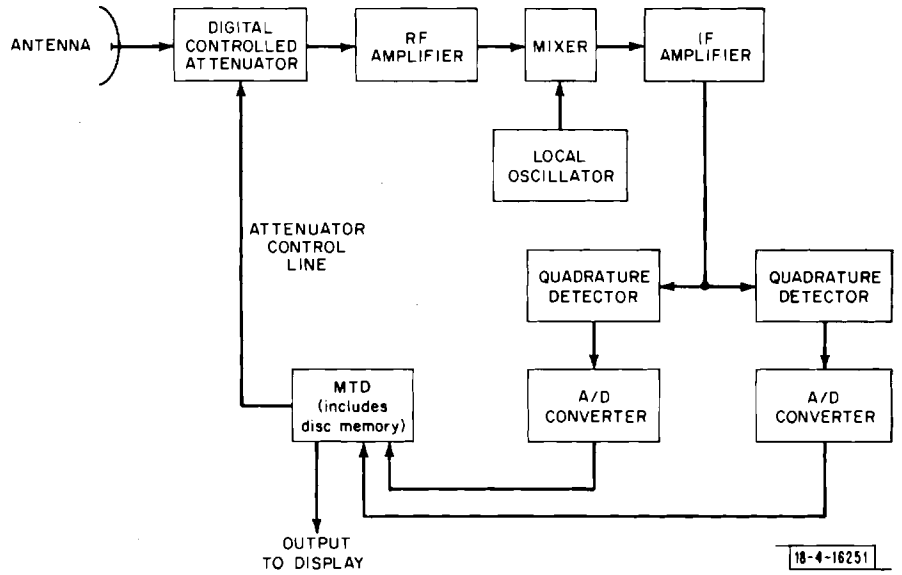

Fig. 7. Feedback Clutter Mapper (FCM) overview.

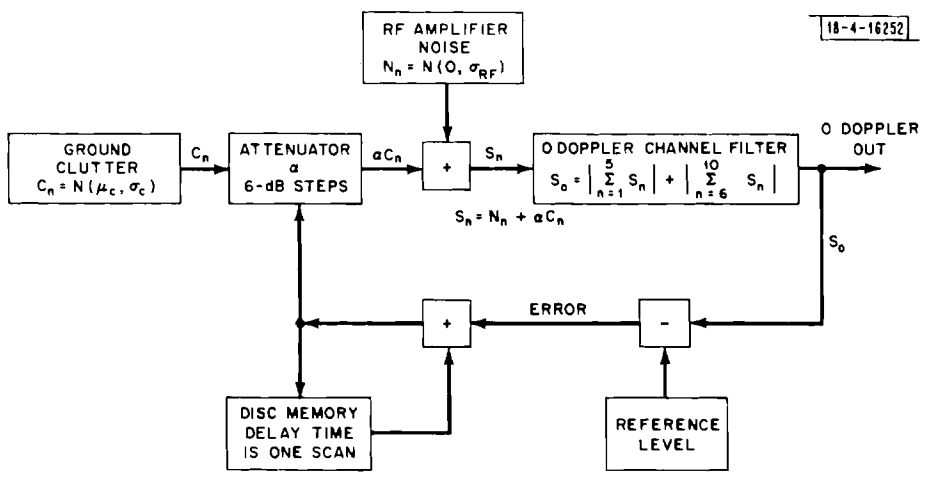

Fig. 8. Feedback Clutter Mapper computer simulation algorithm.

I. Feedback Clutter Mapper (FCM)

Because of the dynamic range limitations of the MTD in its present form, it cannot always achieve its design subclutter visibility (SCV). This fault occurs when the clutter strength is larger than the range of the A/D converters. When saturation occurs, no targets can be detected – weak or strong. Thus, we have a peculiar situation in which the maximum SCV can be achieved only when the clutter level happens to lie just below the saturation level of the A/D converters – a relatively rare event. STC does not cure this problem; it simply reduces the gain of the system so that the average clutter does not saturate. As a result, strong clutter still saturates and potential targets are lost in those areas, while at the same range where there is not clutter, weak targets can be lost because of STC. It is recognized that some STC is needed to eliminate bird clutter, but there are many situations and times when birds are not a concern and the additional sensitivity is useful. Soft limiting can be used to alleviate the problem, but it reduces the SCV whenever the clutter level is high (see 1 December 1973 QTS). It has been proposed that an automated method be employed to adjust the clutter level on a point-by-point basis so that the level is always below saturation. The clutter level at every point (on the PPI) is compared with the desired level (a fixed digital number). If the clutter is too large, attenuation is applied until the clutter approximates the proper level. Conversely, if the clutter is too small, or nonexistent, attenuation is removed until the clutter reaches the desired level or all the attenuation is removed. Digital attenuators are available with adequate response times. This suggests the use of a variation of automatic gain control (AGC) that is commonly used in home receivers. The difference is that each cell of clutter operates independently and the clutter level of each cell is stored individually in a disc memory; hence, the name Feedback Clutter Mapper.

1. Design Considerations

An important feature of the MTD processor is the weather threshold algorithm. Basically, it generates a threshold for the range gate of interest from the average of the weather clutter returns from each of the 16 adjacent range gates (see 1 March 1973 QTS). Weather thresholding is operative in Doppler filters 1 to 7 but not in the zero velocity filter. However, the FCM algorithm has to adjust the attenuator separately for each range cell and, as a consequence, each range-azimuth cell must be weighted appropriately in order to develop the average for the weather threshold. It must be remembered that the attenuator affects all Doppler channels alike. In order to eliminate 16 full-scale weighting multiplies per range gate, it is proposed that the attenuator resolution be limited to a factor of two (6-dB steps). Now the multiplies can be accomplished by sliding a binary decimal point and can easily be implemented in hardware.

Figure 7 is an overview of the pertinent hardware, and Fig. 8 is a diagram of the FCM algorithm. All other aspects of the MTD that do not apply have been eliminated. The incoming clutter power passes through the digitally controlled 6-dB-per-step attenuator and then passes through the front-end RF amplifier where additive zero mean noise is encountered. The signal is first changed to IF, then to quadrature video, and finally sent into the MTD. The zero Doppler filter is implemented by adding five complex returns (S_n) coherently, then taking the sum and adding it to the amplitude of the second set of five,

$$S_o = \left| \sum_{n=1}^{5} S_n \right| + \left| \sum_{n=6}^{10} S_n \right| \quad .$$

TABLE I

Relative Clutter Power (dB)	Zero Doppler S_o (dB)	Sample Standard Deviation ÷ Sample Mean
0	66.4	0.68
20	66.8	0.71
40	65.6	0.53
60	66.7	0.62
80	67.8	0.68

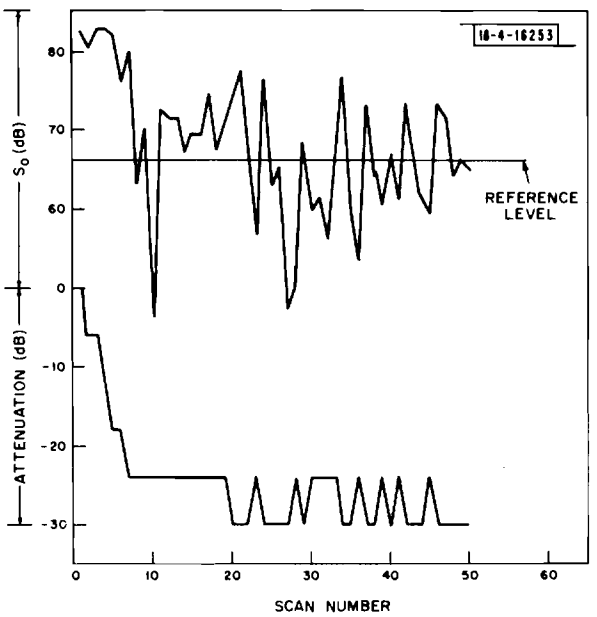

Fig. 9. Feedback Clutter Mapper sample transient response. Saturation of the analog-to-digital converters occurred during the first five scans.

The real number S_o is then compared with a reference level (word) V_o. The error $E = S_o - V_o$ is then fed into an integrator consisting of a disc memory, an adder, and associated buffers which are not shown.

The integrator operates as follows: At the appropriate time, a word representing a clutter map value is read out of the disc memory, the error word is then added algebraically, and the word is returned to memory. The process is repeated for the same word in every antenna scan. The output of the integrator is then truncated to a small integer, n, that runs between 0 and 16 and fed into the attenuator. The 6-dB-per-step attenuator can then be represented by the relation $\alpha = 2^{-n}$ $(n > 0)$, where α is a small fractional number representing the attenuation. The integrator provides the 6-dB/octave roll-off that is needed to maintain stability as provided for in most feedback (servo) loops.

2. Computer Simulation of FCM

Because of the many nonlinear elements in the above feedback loop, it was not practical to predict its performance in an analytical manner. Consequently, a computer program was written to simulate the FCM using Monte Carlo techniques. The input clutter was represented by a computer pseudo-Gaussian random number routine. This routine generates complex Gaussian numbers having a given mean and standard deviation. Thus, the AC portion of the clutter is uncorrelated from scan to scan. The RF amplifier noise is generated similarly and is also uncorrelated but has a zero mean. In this simulation, the RF amplifier noise was set arbitrarily at 40 dB below the saturation level of the A/D converters. The average input clutter level was then cycled through many values while observations were made of the sample mean and sample standard deviation of the zero Doppler filter output S_o. Table I shows some of these results.

Notice that the sample mean of S_o is quite independent of the input clutter power. In fact, there is no upper limit to the input clutter power. We would expect that the fractional fluctuations of S_o, defined as the sample standard deviation of S_o divided by the sample mean of S_o, to be slightly larger than when the attenuator is locked to a fixed setting. Theoretically, this ratio is 0.52. Consequently, it appears that the large 6-dB steps do not contribute very much.

Figure 9 shows what happens when a strong clutter signal is suddenly applied. The upper curve shows how S_o decays to the reference level of 66 dB. It is fairly well stabilized in 15 scans. The lower curve shows the stepping action of the attenuator. Once steady state conditions exist, one can see that the stepping of the attenuator does not contribute much to the fluctuations of S_o. Many sample runs have been made with good results. The simulation includes clutter having a strong DC component present.

3. Conclusions

It appears that the Feedback Clutter Mapper is a possible solution to the problem of adjusting the receiver gain for maximum over-all subclutter visibility without saturating the receiver A/D converters. It is being considered for inclusion in the next version of an MTD-type processor.

J. Stability of Magnetron-Type ASRs

The last QTS (1 December 1973) described initial measurements of the system stability of an ASR-7 radar. Future work calls for the demonstration of radar improvements in the performance of magnetron-type radars by the addition of a digital processor with many of the features of the MTD. To gain full advantage of a new processor, the magnetron-type radar must

have more stability than present operational ASRs. This section describes sources of instability in magnetron-type radars and means of measuring the contributions from each source.

1. Magnetron Stability

The Lincoln Laboratory modified FPS-18 radar uses a coherent klystron amplifier transmitter in order to obtain adequate MTI stability. Since current FAA radars are not so equipped, study has commenced to determine the extent of improvement to subclutter visibility which is achievable with magnetron radars. Magnetron instabilities which do not adversely affect a non-MTI system can be serious in an MTI system, and these defects can not be observed on a conventional spectrum analyzer. Frequency instabilities affect the MTI in the following manner. Consider two point-target returns that are separated by a little less than a pulse length. When these returns arrive at the receiver, the back end of the first pulse is superimposed on the front end of the second pulse. The magnitude of the superposition will depend on the arrival phases. On the next magnetron transmission, the arrival phases (and the magnitude of the superposition) will be different if the second transmission was on a slightly different frequency. The phase difference is given by

$$\Delta\Theta = 2\pi\Delta f T \quad ,$$

where T is the pulse length and Δf is the frequency difference. Thus, if we wish to keep $\Delta\Theta \leqslant 0.01$ (for ~40 dB SCV) the $\Delta f = 0.01/2\pi T = 1592$ Hz for one μsec pulse. The above requirement looks overly severe. However, it must be remembered that it is not FM during the pulse but the change in FM from pulse to pulse that is important.

One way to measure the adequacy of the magnetron stability for MTI processing would be to mix down the pulse to a convenient IF frequency, pass it through a 0.75-μsec delay cable or acoustic delay line, mix it with the undelayed version, and then observe it on a scope. This test separates the short-term pulse-to-pulse instabilities of the magnetron from the rest of the system. Instead of observing the beat on a scope, the output could be digitized and processed on a computer to determine its spectral components, particularly 60 Hz. If 60 Hz is present, steps could be taken to remove it. The magnetron frequency can be "pushed" by modulator hum and poor modulator regulation. The frequency can be "pulled" by variations in the magnetron load, such as the rotating antenna. In general, this will not cause a problem because these fluctuations usually occur at a low frequency.

In recent years, a new class of magnetron has been developed known as the "coaxial magnetron." It has many features that would appear to make it superior to the conventional magnetron for MTI purposes. Because it has a high Q cavity tightly coupled to its vanes, it is expected to be more stable. Conventional spectrum pictures bear this out. Delay-line measurements as described above could determine this stability of such a magnetron. Subjected to properly controlled modulation pulse waveforms, they do not "miss" pulses, mode, or break down as do conventional magnetrons. This is because the energy is stored in the high Q cavity and not between the vanes. It appears to be able to pass the new OTP (Office of Telecommunication Policy) specifications for out-of-band radiation while the conventional tube could not possibly do so.

Finally, one of the manufacturers of coaxial magnetrons indicates substantially longer life for the tube. Thus, an effort should be made to investigate the substitution of this type of tube for current magnetrons. Refitting with coaxial magnetrons will require a minor redesign of the modulator to control the rise time and a mechanical redesign to accommodate its different mechanical dimensions.

2. Coho Stability

A coho generally consists of an LC oscillator which locks on to an input RF pulse. During the time when the pulse is injected, the LC tank has a low Q, enabling the oscillator to lock on to the incoming RF pulse. When the RF pulse ends, the LC tank reverts to a high Q, and the oscillator free runs. The high Q condition of the tank circuit makes the oscillator relatively immune to disturbing influences which may occur during the relatively long period between pulses. Thus, coho tests can be broken down into two parts: lock-on accuracy (error) and frequency stability between pulses.

Ideally, cohos should be solid state devices to minimize disturbing influences such as filament supplies. In addition, the components are small, allowing better isolation against environmental changes.

Tests should be made on the solid state coho used in the ASR-7 to determine whether it is adequate for a high-performance MTI. If not, either a redesign of the unit or procurement of a suitable coho will be necessary.

3. Stalo Stability

As in the coho case above, the ASR-7 stalo should be investigated to determine its suitability for an MTI system. In a coho-magnetron system, it is not necessary for either the stalo or coho to be stable beyond the interpulse period (approximately one millisecond). Since many S-band stalos have been built, it should be possible to replace the ASR-7 unit if it proves unsuitable.

4. Other Stability Problems

It is possible that the various IF and RF amplifiers used in the ASR-7 could prove troublesome by either phase or amplitude modulation of the signals and/or of the reference oscillators. Such problems are generally caused by poor design and are easily corrected.

III. NAFEC SUPPORT (TASK D)

A. Introduction

Task D currently includes support to NAFEC on the following three tasks:

ABIL – Airborne Beacon Interference Locator
TPA – Transponder Performance Analyzer
E-Scan – Electronically Scanned Antenna

Progress on each of these tasks is reported below.

B. Airborne Beacon Interference Locator

During the past quarter, work continued on the development and testing of algorithms to be used for interrogator location and flight-path calculations. Implementation has proceeded using FOCAL,* † a high-level language, in conjunction with assembly language routines interfaced as executable FOCAL functions.

---

* R. Merrill, "FOCAL-11 (Preliminary Version)," DECUS Program 11-24 (16 February 1971).
† "FOCAL Programming Manual," Digital Equipment Corporation, DEC-08-AJAC-0 (April 1969).

1. Software Support

To facilitate the development of programs for the PDP-11, a software package called FOCAL has been introduced. FOCAL is a character-driven interpreter wherein no compilation is necessary for program execution. This has the advantage of allowing on-line editing which permits changes to the algorithms to be implemented very quickly, but results in some loss of computation speed. Execution time has been reduced by coding the most critical real-time functions in assembly language within the framework of FOCAL. The power of the approach has been demonstrated by the short time (one month) required to provide NAFEC with a program for flight-path calculations which support antenna pattern measurements with ABIL.

2. Real-Time Interrogator Location

The real-time interrogator location program is completely coded and partially debugged on local machines. It must next be debugged on the ABIL equipment with real-time data to completely check the timing and interrupt operations.

In the development of the program to do the real-time processing while data are being taken, provision was made for various conditions of overload which may occur. During a normal run, data from the ABIL antenna array and the TACANs are preprocessed in the digital hardware and transferred into a double buffer in the PDP computer for controlled transfer to magnetic tape. The transfer of data from the digital hardware into the buffer and from the buffer to the magnetic tape takes place over direct-access channels with minimal demands on the computer operations. Thus, the real-time program operates in parallel with the loading and unloading operations but must be responsive to interrupts from the data-transfer operation which require computer intervention.

For this real-time operation there are two overflow conditions which must be accommodated without causing the system to hang up. These occur when either the data rate from the hardware processor exceeds that leaving the core buffer or when the parallel processing in the computer cannot keep up with the input data rate. In the first condition, there is no choice but to lose some data. The program will recognize the overflow, inhibit the input of additional data until that already in core is transferred to tape, and then restart data taking. Thus, data segments will be recorded at the maximum capability of the magnetic tape. In the second case, where the parallel processing cannot keep up with the data in real time, all the data will continue to be recorded for after-the-fact processing but the real-time processing will operate for spaced intervals only.

A major portion of the real-time processing involves sorting of the received interrogations into bins representative of the location of the interrogator relative to the aircraft. It was found that computation of the relative azimuth and declination angles of the interrogator for each reply was too time-consuming for real-time operation. In its stead, binning is being done on the basis of raw phase words from the interferometer measurements. If most of the interrogations over the period of a sample come from a few fixed locations, most of the received interrogations will fall into a few bins. These few bins corresponding to given phase words will then be fully processed into relative angular locations, and histograms of the interrogations associated with them will be presented on the output display. If there are many reflected interrogations or if the relative locations of the interrogators change rapidly, a large number of bins will be filled. In these cases, the program will automatically eliminate bins containing fewer than three interrogations.

While the above program has not been fully debugged on the ABIL PDP-11/20, most routines have been successfully run on PDP-11s at M.I.T. The binning algorithm was developed and debugged on the IBM-360 and SEL-86. It is believed that the approach outlined above (use of FOCAL) will hasten the debugging phase and bring it to a speedy conclusion.

3. Flight-Path Calculation

In addition to the interrogator location program just described, NAFEC recently requested an additional program for use when ABIL is measuring antenna patterns. The program would allow on-board determination of a radial from a specified interrogator using ABIL TACAN data.

The inputs to this program are the latitude and longitude of the three TACAN stations and the interrogator of interest. Also, the magnetic deviation and aircraft altitude must be entered. The program will continually calculate the azimuth and range from the interrogator to the aircraft and the aircraft heading to fly to the interrogator, permitting real-time control of aircraft flight path to facilitate the measurement process. The algorithm uses the west-most TACAN as a reference to save computation time in resolving angle ambiguities.

The program has been coded in FOCAL in much the same manner as the interrogator location program and successfully executed on two PDP-11/40s and a PDP-8 using simulated TACAN data.

C. Transponder Performance Analyzer

Work in support of TPA continued in the areas of data analysis and software development. The magnetic tape containing individual ATCRBS replies, which was recorded by TPA in September 1973, was further processed and examined. The program for conversion of tape data to a printed format amenable to analysis was modified to allow selected replies to be output while all others were inhibited.

The tape was examined for false targets caused by multipath reflection. During the entire 50 scans of data there was only a single instance of replies being received from a given aircraft on two different azimuths, which would be indicative of a reflected false target. However, there was no reflecting surface in the position required to cause the false target. It was concluded that the reply sequence was not that of a false target but was probably caused by synchronous garbling of an aircraft code. No other false targets were noted in the data; this is better than usually observed at ASR installations, but is not surprising considering the lack of large tall buildings in the vicinity of the TPA antenna.

Since the TPA data were recorded without a defruiter, an estimate of fruit generation could be made and the identity of interrogators established. From analysis of this data, over 20 different interrogators have been identified as responsible for fruit seen by the TPA. Analyses of data from ARTS-III sites have shown a capability to also determine interrogator prf, scan rate, and location from such undefruited data.

Programming work has begun on an algorithm to process TPA data to determine automatically the presence of multipath-induced false targets and calculate the parameters of the reflecting surfaces responsible. The first and most complex portion of this algorithm is to produce target reports from reply data. This is being developed from several previously available algorithms for target declaration and is being tailored to the particular parameters of the TPA. Since target reports are directly available in ARTS extraction tapes, this second algorithm can be used to determine false-target reflectors for ARTS sites.

Analysis of data from ARTS-III sites has continued at a low level of effort. The major portion of ARTS-III data analysis work done during this reporting period was performed for the U.S. Air Force and is briefly described here because it appears directly applicable to widespread FAA problems. A study was made of the ARTS-III/ATCRBS environment at Kirtland Air Force Base/Albuquerque International Airport, New Mexico, using ARTS-III extracted data tapes, to determine the extent of the current false-target problem and to predict the effects on system performance of the construction of a new hangar near the interrogator. Based on this analysis, it was concluded that severe reflection problems exist and that the new building would probably not aggravate the situation further.

To address the basic problem, two software processing techniques were developed for possible inclusion in the ARTS-III enhancement program. These techniques are described in Lincoln Laboratory Technical Note 1974-12, "False Target Elimination at Albuquerque Using ARTS-III Software." Briefly, these techniques rely on the observed highly deterministic relationship between the apparent position of a false target and the actual position of the aircraft causing it. Whenever an aircraft enters a region of airspace which is illuminated by a reflecting surface, the location at which a resulting false target would occur is searched for a new target agreeing in altitude and code. Steps are taken to identify any such new targets as false, depending on the extent of agreement.

D. E-Scan Antenna

During this reporting period, a number of detailed analyses preparatory to the field environment tests were carried out and furnished to the program manager. In addition, specific recommendations concerning the measurements were made. Finally, we participated actively in a working group comprising representatives of ANA-120, RD-241, Hazeltine, and Lincoln Laboratory to develop and produce a new test plan.

Preliminary analysis of false targets expected to be produced by reflections from the maintenance hangar (Building 301) has been made to provide guidance for planning quantitative measurements with efficient utilization of aircraft. As with antenna pattern measurements at 1030 MHz, instrumentation is required for identifying the desired interrogation and for measuring and recording amplitudes of the P2 and P3 pulses. Two pragmatic kinds of results are also sought from these tests: how does the E-scan compare with the standard ATCRBS antenna in producing false targets, and how well does beam-lift avoid producing false targets? Some preliminary tests indicate that most of the false targets produced by the standard antenna at the RBTF would not be produced by the E-scan. In fact, only Building 301 has thus far been observed to act as an effective reflector for the E-scan beam. Moreover, it has been observed that the 4° lift successfully prevents appearance of those false targets.

Because Building 301 is extremely atypical, evaluation of the merits of E-scan, with and without beam-lift, for solving false target problems at other locations will depend on obtaining better models for the various reflecting surfaces encountered elsewhere.

It has been proposed that airborne pulse amplitude measurements include gathering data in and near the shadow region produced by Building 301 to test predictions based on knife-edge diffraction. Analysis indicates that a fading of 14 dB would be expected for an aircraft at a distance of 12 nmi and an altitude of 2500 ft; this would persist for seven to eight scans. If the beam were lifted 2° or 4°, the fading would be greater by 4 or 8 dB, respectively.

A complete review of the site tests was accomplished by the working group which met continuously from 4 to 22 February. Most of the discussions concerned techniques and procedures to obtain quantitative data during the various tests within the limits of available time and resources. Computations and analyses are continuing in order to optimize these tests. Testing is expected to commence in the near future.

IV. PRECISION ALTITUDE LANDING MONITOR (TASK E)

A. Introduction

Construction of the PALM experimental system has been completed during this quarter. Testing of the three major subsystems (antenna, receiver, and timing and control) and integration of the full system have been accomplished. The antenna system has been installed at the

Fig. 10. PALM test facility.

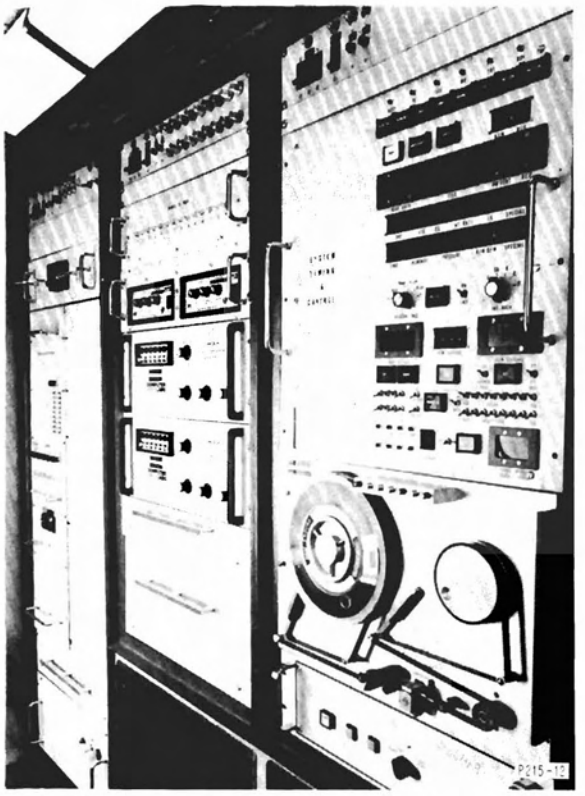

Fig. 11. Processing equipment installed in instrumentation van.

Lincoln Laboratory Antenna Range and the instrumentation system (receiver and timing and control) has been installed in the mobile test van (Fig. 10). An over-all view of the instrumentation system within the van is shown in Fig. 11.

During the next quarter, feasibility testing using fixed far-field and near-field reference sources will be conducted.

B. Antenna Subsystem

The PALM antennas were received during this quarter. Extensive tests of each antenna were conducted in the Laboratory's anechoic test chamber. The results of these tests indicate that the antennas meet or exceed the important PALM performance requirements.

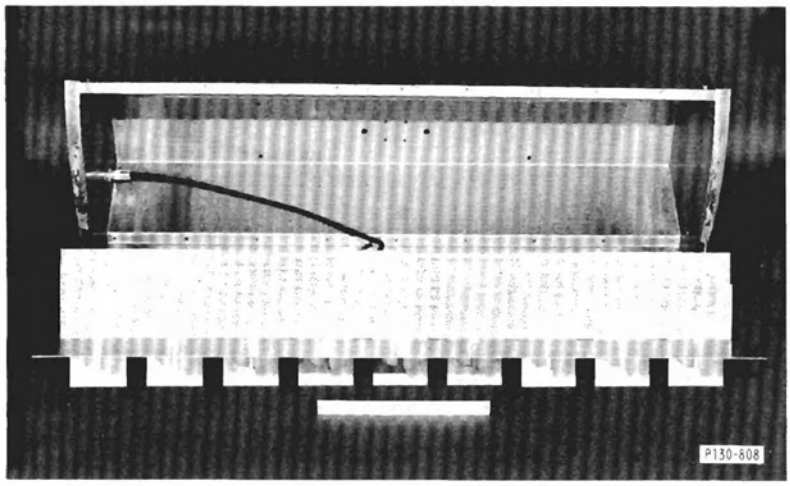

Fig. 12. Antenna feed network.

The desired antenna pattern* was synthesized using a procedure based on techniques which grew out of digital filter design. The antennas have been fabricated using printed circuit techniques with stripline feeds (Fig. 12). The patterns for the five antennas used in the PALM array are illustrated in Figs. 13(a) through 13(e) and indicate a close match over the coverage region. The five antennas have been aligned on the vertical support (Fig. 10) to make the gain at the horizon 12 ± 0.2 dB down from the peak gain. The measurements indicate that within the band 1090 ± 3 MHz,

Gain = 15.3 ± 0.5 dB,
VSWR $\leqslant$ 1.2,
Cross polarization isolation $\geqslant$ 20 dB in the 1° to 40° elevation region.

The spacing between adjacent antenna pairs has been selected to be $17\lambda/3$, $17\lambda/3$, $17\lambda/3$ and $17\lambda/2$. Precise differential separation of the antennas has not been accomplished at this time since it will not be a factor in the system error budget for early low-angle measurements. The present errors will introduce less than 1 mrad of estimation error at 30° true elevation and negligible error near the test elevation region (0.5° to 1.5°).

C. Receiving System

The receiving system has been under test throughout this reporting period, and the four measurement channels have been matched to the reference channel in amplitude and phase. Channel differential amplitude and phase response, as a function of frequency, are shown in

* "ATC Surveillance/Communication Analysis and Planning," Quarterly Technical Summary, FAA-RD-73-161, Lincoln Laboratory, M.I.T. (1 September 1973).

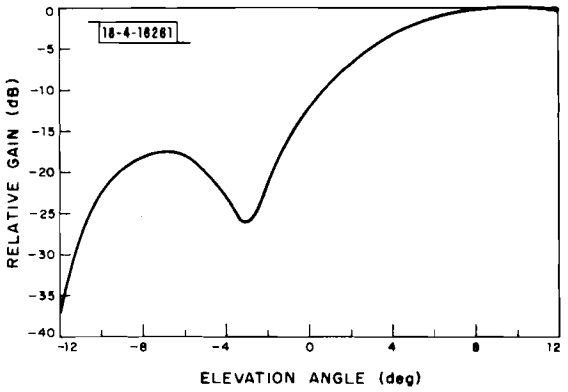

(a) Antenna No. 5. Reference antenna.

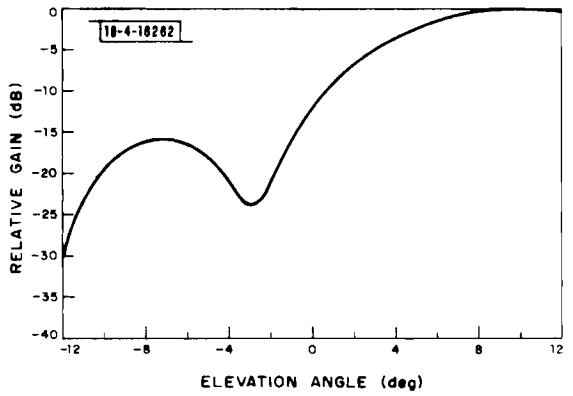

(b) Antenna No. 2. Second antenna 17λ/3 above reference.

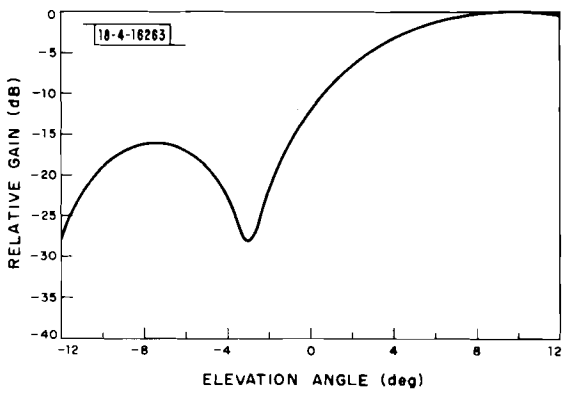

(c) Antenna No. 4. Third antenna 34λ/3 above reference.

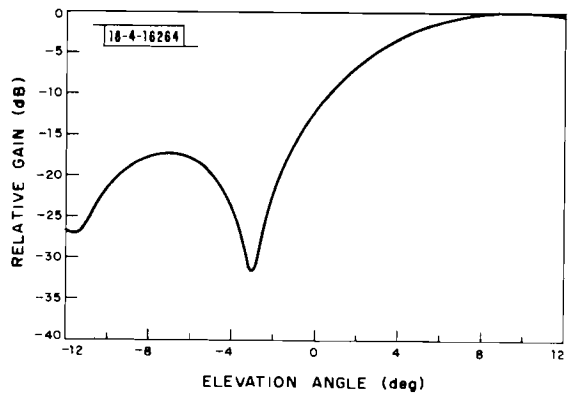

(d) Antenna No. 3. Fourth antenna 17λ above reference.

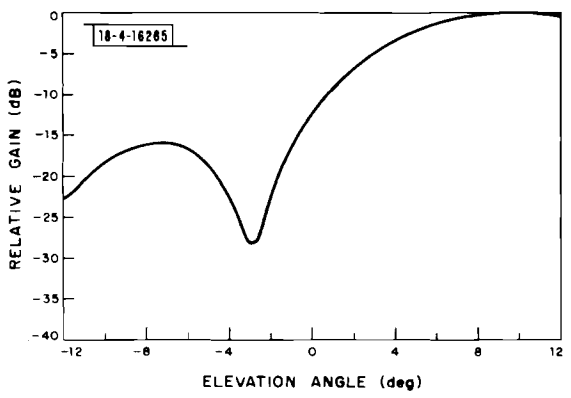

(e) Antenna No. 6. Fifth antenna 25.5λ above reference.

Fig. 13. Elevation patterns.

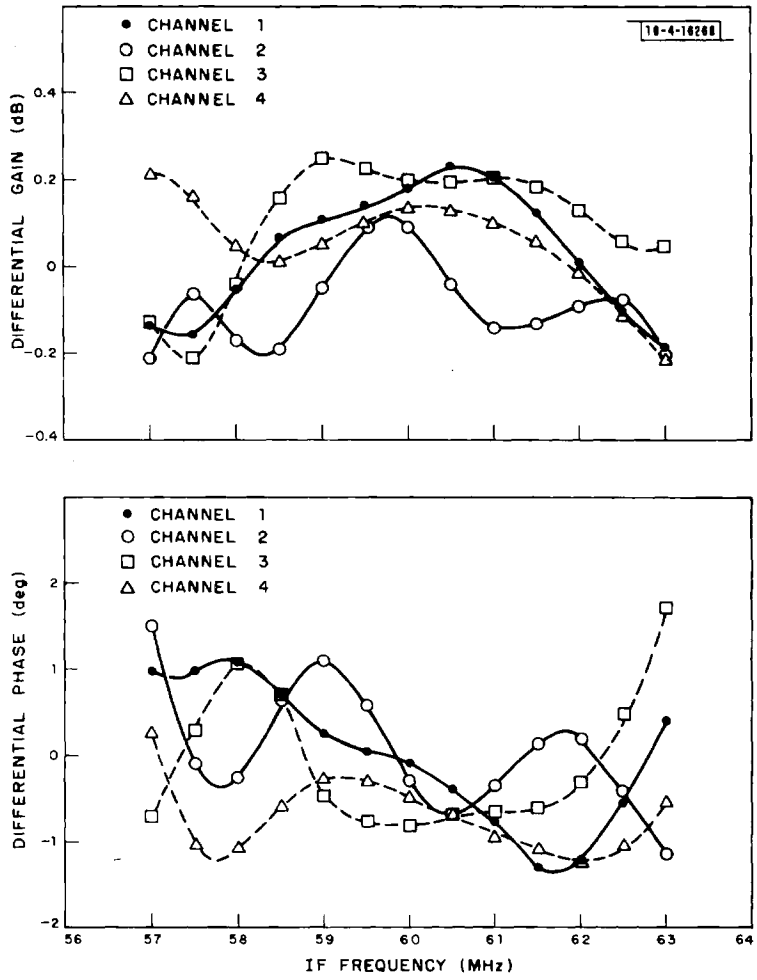

Fig. 14. Channel differential amplitude and phase response.

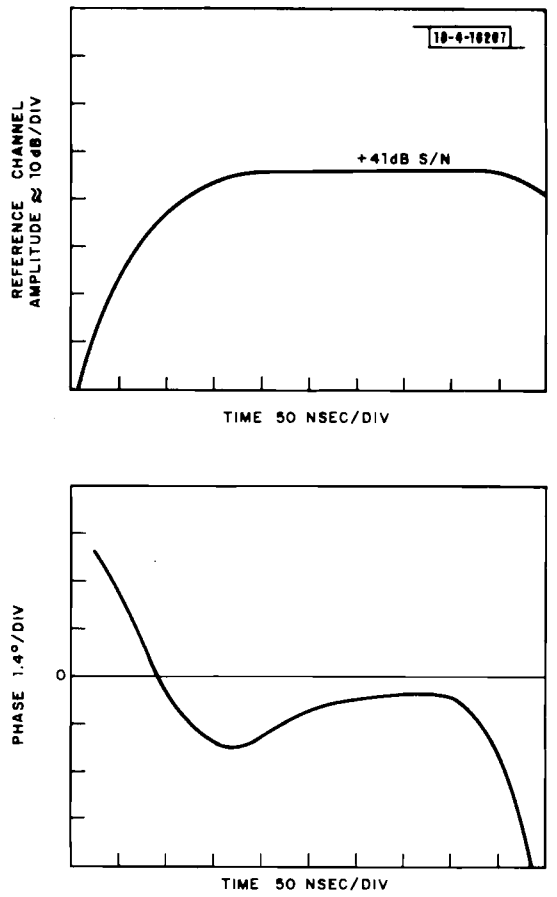

Fig. 15. Transient amplitude and phase response.

Fig. 14. A typical channel transient amplitude and phase response to a 450-nsec pulse at 1090 MHz is shown in Fig. 15. Measurements of channel precision and stability are under way; results to date indicate that differential channel phase measurements hold to within ±1° over a 24-hour period.

D. Timing and Control System

The timing and control system was completed during this quarter, and all measurement features have been designed. The auxiliary data channels have not been checked out at this time since they will not be required until live tests with aircraft begin later this year. The system is installed in the mobile facility and is supporting full system testing.